A framework for quantifying the impacts of climate change and human activities on hydrological drought in a semiarid basin of Northern China

Running head: *Impacts of climate change and human activities on hydrological drought*

Shanhu Jiang [a,b], Menghao Wang [a,b,*], Liliang Ren [a,b,*], Chong-Yu Xu[c], Fei Yuan [a,b], Yi Liu[a], Yujie Lu [a,b], Hongren Shen[d]

a. State Key Laboratory of Hydrology-Water Resources and Hydraulic Engineering, Hohai University, Nanjing, China

b. College of Hydrology and Water Resources, Hohai University, Nanjing, China

c. Department of Geosciences, University of Oslo, N-0316 Oslo 1047 Blindern, Norway

d. Department of Civil and Environmental Engineering, University of Waterloo, Waterloo N2L3G1, Canada

*Corresponding Author: Liliang Ren, Menghao Wang

*Corresponding author at: State Key Laboratory of Hydrology-Water Resources and Hydraulic Engineering, Hohai University, Nanjing 210098, China.

E-mail address: njrll9999@126.com; wmh0331@126.com

This article has been accepted for publication and undergone full peer review but has not been through the copyediting, typesetting, pagination and proofreading process which may lead to differences between this version and the Version of Record. Please cite this article as doi: 10.1002/hyp.13386

Abstract

Climate change and human activities are two major driving forces affecting the hydrologic cycle, which further influence the stationarity of the hydrologic regime. Hydrological drought is a substantial negative deviation from the normal hydrologic conditions affected by these two phenomena. In this study, we propose a framework for quantifying the effects of climate change and human activities on hydrological drought. First, trend analysis and change point test are performed to determine variations of hydrological variables. After that, the fixed runoff Threshold Level Method (TLM) and the Standardized Runoff Index (SRI) are used to verify whether the traditional assessment methods for hydrological drought are applicable in a changing environment. Finally, two improved drought assessment methods, the variable TLM (TLM_v) and the SRI based on parameter transplantation (SRI_t) are employed to quantify the impacts of climate change and human activities on hydrological drought based on the reconstructed natural runoff series obtained using the Variable Infiltration Capacity (VIC) hydrologic model. The results of a case study on the typical semiarid Laohahe basin in North China show that the stationarity of the hydrological processes in the basin is destroyed by human activities (an obvious change-point for runoff series is identified in 1979). The traditional hydrological drought assessment methods can no longer be applied to the period of 1980–2015. In contrast, the proposed separation framework is able to quantify the contributions of climate change and human activities to hydrological drought during the above period. Their ranges of contributions to hydrological drought calculated by the TLM_v method are 20.6–41.2% and 58.8–79.4%, and the results determined by the SRI_t method are 15.3–45.3% and 54.7–84.7%, respectively. It is concluded that human activities have a dominant effect on hydrological drought in the study region. The novelty of the study is twofold. First, the proposed method is demonstrated to be efficient in quantifying the effects of climate change and human activities on hydrological drought. Second, the findings of this study can be used for hydrological drought assessment and water resource management in water-stressed regions under non-stationary conditions.

Keywords: Hydrological drought; Human activities; Climate change; Standardized Runoff Index; Threshold Level Method

1. Introduction

Droughts affect both the surface and ground water resources and can significantly reduce the existing water supplies, deteriorate water quality, and reduce crop productivity, as well as affect a host of social and economic activities (Heim, 2002; Dai, 2011; Rivera et al., 2018). According to various types of water deficits (e.g. precipitation, streamflow, soil moisture content and water resources), droughts can be classified into four major types: meteorological, agricultural, hydrological, and social-economical (Mishra and Singh, 2010; Ma et al., 2014; Ye et al., 2016). Hydrological drought, which can be defined as inadequate surface and subsurface water resources for established water uses of given water resources management system, is considered one of the most important types of drought (Shukla and Wood, 2008; Van Loon, 2015). In particular, assessing hydrological drought in a changing environment is important for drought disaster management.

Climate change is expected to affect the manifestation of terrestrial extreme phenomena such as droughts (Sheffield et al., 2012; Li et al., 2017; Haro-Monteagudo et al., 2018). For instance, the changes of precipitation and evapotranspiration are likely to affect the evolution characteristics of droughts (Vicente-Serrano et al., 2015). Due to the enhanced evapotranspiration (caused by rising temperatures) without increasing precipitation, higher frequency and magnitude of the hydrological drought risk have been predicted for the coming century in most locations over the world (Sheffield et al., 2012; Dai, 2013; Trenberth et al., 2014). However, the impact factors of droughts are not limited to climate change, human activities are also the main driving forces affecting hydrological drought (Van Loon and Van Lanen, 2013). Human activities in forms of land cover change, agricultural irrigation, water extraction, and reservoir regulation influence the processes of the hydrological cycle, and further affect the variability characteristics of hydrological drought (Ren et al., 2002; Han et al., 2014; Van Loon et al., 2016; Zhu et al., 2018). For example, He et al. (2017) and Zhang et al. (2018) conducted that human water management has intensified the hydrological drought in California and Yangtze River, respectively. Thus, in this climate change and human activities

comprehensively influenced era, scientific cognition of the effects of climate change and human activities on hydrological drought has become a new challenge.

To date, there have been some studies itemized for analysis of the effects of climate change and human activities on hydrological drought, in which the assessments of climate change impacts are mainly based on the drought indices evaluation considering the changes of meteorological conditions (Sheffield et al., 2012; Dai, 2013; Trenberth et al., 2014; Yu et al., 2014; Zhu et al., 2016; Wang et al., 2018; Safavi et al., 2018), while the studies of human activities impacts are mainly based on the watersheds comparative analysis and natural runoff reconstruction (Wan et al., 2017; He et al., 2017; Zhang et al., 2018; Bazrafshan and Hejabi, 2018; Tijdeman et al., 2018; Firoz et al., 2018). For instance, Wang et al. (2018) evaluated the spatiotemporal variation of future drought (2016–2100) in the Pearl River Basin (PRB) in South China and found that climate change enhances the severity and variability of drought in the PRB in the 21st century. Tijdeman et al. (2018) quantified the impact of the human activities on the streamflow drought by comparing the dataset consisting of catchments with near-natural flow as well as catchments for which different human influences indicated in the metadata. Compared with the itemized impact assessment, there are only a few investigations comprehensively analyzed the effects of climate change and human activities on hydrological drought (Van Loon and Van Lanen, 2013; Liu et al., 2016; Ren et al., 2016; Lin et al., 2017). Van Loon and Van Lanen (2013) proposed a quantitative discrimination framework for drought (natural driving) and water scarcity (human driving) using an observation-modeling method. Liu et al. (2016) analyzed the connections between meteorological and hydrological droughts of the Laohahe basin by a fixed runoff Threshold Level Method (TLM). Ren et al. (2016) evaluated hydrological drought evolution characteristics over the Weihe catchment using the Standardized Runoff Index (SRI) with a time-variant parameterization scheme. However, these studies either used only one method (or index) or failed to quantitatively distinguish the effects of climate change and human activities on hydrological drought. Thus, the objective of this study is to construct a framework for quantifying the impacts of climate change and human activities on hydrological drought, comprehensively using two different methods: the variable

TLM (TLM_v) and the SRI based on parameter transplantation (SRI_t).

The Laohahe basin is a highly human-impacted watershed in the Northern part of China, with hydrological drought occurring frequently (Liu et al., 2009; Jiang et al., 2011). The proposed framework will be adopted to quantify the effects of climate change and human activities on hydrological drought in Laohahe basin and the research results are important for the local drought disaster mitigation and sustainable development of water resources.

2. Materials and methods

2.1. Study area

The Laohahe catchment (41°N–42.75°N, 117.25°E–120°E) located in the northern China (Fig. 1) covers a drainage area of 18112 km^2. The climate is semiarid, and the elevation ranges between 427 m and 2054 m a.m.s.l. with a generally increasing trend from the northeast to the southwest. The long-term mean annual air temperature, precipitation, and runoff observed in the period between 1964 and 2015 are 7.57°C, 417.9 mm, and 24.9 mm, respectively. The Laohahe catchment exhibits strong seasonality of runoff because of the uneven precipitation distribution (80% of the annual precipitation occurs between May and September).

2.2. Data

The data used in this study are as follows:

(1) Daily precipitation data measured by 52 rain gauges and streamflow records of the Xinglongpo hydrological station for the period of 1964–2015 are provided by the Water Resources Department of the Inner Mongolia Autonomous Region. Streamflow data are further converted to catchment runoff by averaging the runoff amounts over the catchment area to compare with the precipitation and potential evapotranspiration (PET), which was calculated via the Penman-Monteith equation recommended by FAO (Allen et al., 1998).

(2) Daily meteorological forcing data (1964–2015) including the maximum and minimum air temperature, wind speed, relative humidity, and sunshine duration measured by three national standard meteorological stations inside and around the Laohahe catchment are downloaded from the China Meteorological Data Sharing Service System (http://data.cma.cn/).

(3) Geographic information is obtained as follows. Soil types are derived from the Food and Agriculture Organization (FAO) dataset, and vegetation types are obtained from the University of Maryland's 1 km Global Land Cover Production. The 30 arc-second global digital elevation model (GTOPO30) data are obtained from the U.S. Geological Survey (USGS), and re-sample to $0.0625° \times 0.0625°$ resolution to generate flow directions, basin mask, and contributing areas for running the Variable Infiltration Capacity (VIC) model (Liang et al., 1994).

(4) Socioeconomic statistical information for Chifeng city in the Laohahe basin regarding the gross domestic product (GDP), food production, population, and livestock is collected from a local statistical bureau website.

2.3. Trend and change-point analysis

2.3.1. Mann-Kendall test

The Mann-Kendall (MK) test is a non-parametric test method recommended by the World Meteorological Organization (WMO) and widely used to determine trends of data series. It is applicable to the analysis of non-normal distribution data such as hydrologic and meteorological series. For a time series $X = \{x_1, x_2, \cdots, x_n\}$ with $n > 10$, the standard normal statistic Z is estimated as follows:

$$Z = \begin{cases} (S-1)/\sqrt{\mathrm{var}(S)} & S > 0 \\ 0 & S = 0 \\ (S+1)/\sqrt{\mathrm{var}(S)} & S < 0 \end{cases} \quad (1)$$

where

$$S = \sum_{i=1}^{n-1} \sum_{j=i+1}^{n} \mathrm{sgn}(x_j - x_i) \quad (2)$$

$$\mathrm{sgn}(\theta) = \begin{cases} +1 & \theta > 0 \\ 0 & \theta = 0 \\ -1 & \theta < 0 \end{cases} \quad (3)$$

$$\mathrm{var}(S) = \left[n(n-1)(2n+5) - \sum_t t(t-1)(2t+5) \right] / 18 \quad (4)$$

where t is the extent of any given tie, and $\sum_t$ denotes the summation of all ties. The

statistic Z follows the standard normal distribution. At a 5% significance level, the null hypothesis of no trend is rejected if |Z| > 1.96. A positive value of Z denotes an increasing trend, and the opposite corresponds to a decreasing trend (Mann, 1945; Kendall, 1975).

2.3.2. Pettitt test

The Pettitt test is a non-parametric test method used to determine the occurrence of a change-point at a given significance level, which is based on rank statistics and independent of distribution. This method is widely used to analyze the change-point of hydrological and meteorological variables.

This approach considers a time series as two samples represented by $x_1,\cdots,x_t$ and $x_{t+1},\cdots,x_N$. The Pettitt indices $U_{t,N}$ can be calculated from the following formula (Pettitt, 1979; Kiely et al., 1998):

$$U_{t,N}=\sum_{j=1}^{t}\sum_{i=1}^{N}\operatorname{sgn}\left(x_j-x_i\right)\qquad\left(t=1,\cdots,N\right) \tag{5}$$

where

$$\operatorname{sgn}\left(\theta\right)=\begin{cases}+1 & \theta>0\\ 0 & \theta=0\\ -1 & \theta<0\end{cases} \tag{6}$$

Then, we can calculate the series of probabilities of change-points for each year by the following formula (Kiely et al., 1998):

$$P\cong 1-\exp\left[\frac{-6\left(U_{t,N}\right)^2}{N^3+N^2}\right] \tag{7}$$

2.3.3. Precipitation-runoff double cumulative curve method

The precipitation-runoff double cumulative curve (DCC) method can visually illustrate the consistency of precipitation and runoff data (Jiang et al., 2012a). Normally, it is represented by a straight line, and the change in the gradient of the curve may infer that the characteristics of precipitation or runoff have changed. In this study, the DCC method was utilized for the auxiliary detection of the change-point of the runoff series.

2.4. Framework for quantifying the effects of the climate change and human activities

Distinguishing droughts induced by different factors is essential for objective understanding the underlying causes of regional drought, which is also important for water planning and management. In this section, a framework is developed to quantify the effects of climate change and human activities (Fig. 2), which assumes climate change and human activities to be independent factors affecting hydrological drought. This assumption allows a linear and additive relationship between the relative contributions of climate change and human activities.

The proposed framework can be divided into three sections. (1) In the first step, a change-point is determined from the hydrometeorological variables. After that, the entire period can be divided into two parts: the baseline period ("undisturbed") and change period ("disturbed"). For change-point detection, the Pettitt test and DCC method are selected. (2) The second step focuses on reconstructing the runoff series of the change period by the hydrologic model, which is first calibrated via hydrometeorological forcing data during the baseline period. After that, while keeping the optimized parameters constant, the meteorological forcing of the change period is used to reconstruct (simulate) the runoff series without involving human activities. Hydrological models can be used to reproduce the natural flow situation; in this study, the distributed VIC model is used for this purpose (its detailed description is provided in the following section). (3) The third step is the core of this framework. The effects of climate change and human activities on hydrological drought during the change period can be quantitatively determined by identifying the observed and simulated runoff series using the TLM_v method and the SRI_t method, respectively. The hydrological drought identified by the observed runoff series are affected by both climate change and human activities, while the latter are developed at the natural conditions (affected only by climate change). Thus, their difference represents the droughts caused exclusively by human activities.

2.4.1. Variable runoff Threshold Level Method

The TLM is the most commonly used approach for studying hydrological droughts (Van Loon and Van Lanen, 2013; Liu et al., 2016; Razmkhah, 2017; Sarailidis et al., 2018). According to this method, drought events occur when the flow is below a predefined threshold Q_z (Fig. 3a). Each event can be characterized by some measure of severity, such as the deficit volume, v_k, (calculated by summing up the differences between the actual flux and threshold level over a specified period), time of occurrence, t_k, drought duration, d_k, and drought interval, i_k, (the time period between two consecutive drought events).

The selection of threshold Q_z is subjective but essential since it influences the number of events, drought duration, and deficit volume. In this study, the TLM_v is utilized to represent strong seasonal variability. A monthly threshold derived from the 70th percentile of the monthly duration curves was used, which implied that the selected runoff value for each month was equal to or exceeded 70% of the time in that specific month. The variable threshold values were calculated from the baseline period and then applied to the change period. Different threshold values were computed for the observed and simulated runoff series to reduce the influence of the simulation error.

We selected the deficit volume (v_k) from the TLM_v method to separate the effects of different factors on hydrological drought. In particular, v_{total} was used to represent the total impact on hydrological drought caused by both climate change and human activities, which was calculated by summing up the differences between the observed series and the threshold values obtained for the baseline period. v_{recon} was used to represent the impact on hydrological drought caused by climate change, which was calculated by summing up the differences between the simulated series and the threshold values (determined for the baseline period). In addition, the difference between v_{total} and v_{recon} (denoted as v_{human}) represents the effects of human activities. The relative contributions (i.e., percentages) of climate change (I_c) and human activities (I_h) to hydrological drought can be defined as follows:

$$I_c = \frac{v_{recon}}{|v_{human}| + |v_{recon}|} \times 100\% \quad (11)$$

$$I_h = \frac{v_{human}}{|v_{human}| + |v_{recon}|} \times 100\% \quad (12)$$

The runoff series were examined at a moving average of 3 months to make the TLM_v method comparable to the SRI_t method on the time scale.

2.4.2. The Standardized Runoff Index based on parameter transplantation

The SRI was used as the useful counterpart for depicting the hydrological aspects of drought (Shukla and Wood, 2008). The long-term streamflow series were first fitted to the probability distribution function (Nalbantis and Tsakiris, 2009; Ren et al., 2016). Once the distribution was determined, the cumulative probability was then transformed to the standard normal SRI value using the following approximation:

$$SRI = \begin{cases} -\left(t - \dfrac{C_0 + C_1 t + C_2 t^2}{1 + d_1 t + d_2 t^2 + d_3 t^3}\right), & t = \sqrt{\ln\left(\dfrac{1}{\left[F(x)\right]^2}\right)}, \quad 0 < F(x) \le 0.5 \\ t - \dfrac{C_0 + C_1 t + C_2 t^2}{1 + d_1 t + d_2 t^2 + d_3 t^3}, & t = \sqrt{\ln\left(\dfrac{1}{\left[1 - F(x)\right]^2}\right)}, \quad 0.5 < F(x) < 1 \end{cases} \quad (8)$$

where $F(x)$ is the cumulative distribution function, and the constants are defined as C_0 = 2.515517, C_1 = 0.802853, C_2 = 0.010328, d_1 = 1.432788, d_2 = 0.189269, and d_3 = 0.001308.

After that, the SRI value is used to determine whether a drought event has occurred (Fig. 3b) and obtain the drought characteristics (e.g. time of occurrence, t_k, duration, d_k, drought severity, s_k, and drought interval, i_k). In this study, the drought severity can be divided into five classes based on the SRI values: non-drought when $SRI > -0.5$, mild drought when $-1.0 < SRI \le -0.5$, moderate drought when $-1.5 < SRI \le -1.0$, severe drought when $-2.0 < SRI \le -1.5$, and extreme drought when $SRI \le -2$. Specially $SRI > -0.5$ was defined as the normal range to reduce the number of "minor drought" events without affecting the drought rating.

The calculation core of the SRI method is fitting the runoff series with an appropriate probability distribution function under the assumption of stationarity. However, under the effects of both climate change and human activities, this assumption may no longer be valid for many river basins, making the corresponding model or method not applicable under

non-stationary conditions.

In this study, a parameter transplant method was used to construct a new SRI series (denoted as SRI_t) to represent the total change of the hydrological drought caused by both climate change and human activities. Through the optimization of the probability distribution function, a three-parameter generalized extreme value (GEV) distribution function that passed the Kolmogorov-Smirnov test was used to fit the runoff series in the baseline period (the effects of human activities on hydrological drought were less recognized during this period). After that, the parameters and distribution of the probability function were extracted and transferred to the observed and simulated runoff series during the change period to calculate the SRI series, respectively. The SRI values determined from the observed series (SRI_t) during this period represent the total change in hydrological drought caused by both climate change and human activities. Further, the SRI values computed from the reconstructed (simulated) series (SRI_r) during the change period represent the changes in hydrological drought caused by climate change. Therefore, the difference between SRI_t and SRI_r (denoted as SRI_h) represents the effects of human activities. The relative contributions (i.e., percentages) of climate change (I_c) and human activities (I_h) to hydrological drought can be defined as follows:

$$I_c = \frac{SRI_r}{|SRI_h| + |SRI_r|} \times 100\% \quad (9)$$

$$I_h = \frac{SRI_h}{|SRI_h| + |SRI_r|} \times 100\% \quad (10)$$

Here, the SRI series corresponding to the 3-month time scale ($SRI\text{-}3_t$) was selected for the quantitative analysis of hydrological drought.

2.4.3. The VIC hydrologic model

VIC is a macro-scale distributed hydrologic model that balances both the water and surface energy budgets. By dividing the land surface into different land-cover types and bare soil, it incorporates the sub-grid spatial change of precipitation and infiltration (Liang et al., 2004). The model parameters can be classified into two categories. The first category of

parameters is not adjusted once determined (e.g. the saturated soil potential ψ_s (m), soil porosity θ_s ($m^3 \cdot m^{-3}$), and saturated hydraulic conductivity k_{sat} (ms^{-1})) and the classifications of the University of Maryland global land cover (e.g. root depth and fraction). Another category includes seven user-calibrated parameters (listed in Table 1), in which *B* (the infiltration curve parameter) and d_2 (the thickness of the middle soil moisture layer) are the two most sensitive ones.

In this study, the VIC model was implemented from 1964 to 2015 using a 24-h temporal and $0.0625° \times 0.0625°$ spatial resolution. The Muskingum method was employed as the streamflow routing module to produce a model-simulated runoff at the Xinlongpo hydrologic station. The coefficient of correlation (CC), Nash-Sutcliffe efficiency coefficient (NSE), and relative error (BIAS) specified by Equations (13), (14), and (15), respectively, were used to evaluate the model performance (Jiang et al., 2012b; Jiang et al., 2018b).

$$CC = \frac{\sum_{i=1}^{n}\left(Q_{obs}(i) - \bar{Q}_{obs}\right)\cdot\left(Q_{sim}(i) - \bar{Q}_{sim}\right)}{\sqrt{\sum_{i=1}^{n}\left(Q_{obs}(i) - \bar{Q}_{obs}\right)^2}\sqrt{\sum_{i=1}^{n}\left(Q_{sim}(i) - \bar{Q}_{sim}\right)^2}} \tag{13}$$

$$NSE = 1 - \frac{\sum_{i=1}^{n}\left(Q_{sim}(i) - Q_{obs}(i)\right)^2}{\sum_{i=1}^{n}\left(Q_{obs}(i) - \bar{Q}_{obs}\right)^2} \tag{14}$$

$$BIAS = \frac{\sum_{i=1}^{n}\left(Q_{sim}(i) - Q_{obs}(i)\right)}{\sum_{i=1}^{n} Q_{obs}(i)} \tag{15}$$

where $Q_{obs}(i)$ is the observed runoff (mm/month) at time step *i*, $Q_{sim}(i)$ is the simulated runoff (mm/month) at time step *i*, $\bar{Q}_{obs}$ is the mean observed runoff value (mm/month), $\bar{Q}_{sim}$ is the mean simulated runoff value (mm/month), and *n* is the number of data points.

3. Results and Discussion

3.1. Hydrological variation analysis

Firstly, the precipitation, PET, and runoff series obtained over the Laohahe catchment from 1964 to 2015 were analyzed. According to Fig. 4a, Fig. 4b, and Fig. 4c, the precipitation and PET series show slightly decreasing trend during the past 52 years, whereas the runoff series exhibits a rapidly decreasing trend with a large descending rate. More directly, we analyzed the inconsistent change of the precipitation and runoff series using runoff coefficient (Fig. 4d). Its mean value in the basin was 0.06, but during the three dry decades (1980s, 2000s, and 2010s), the runoff coefficient was extremely low (significantly less than 0.06). In addition, the MK test was performed for the trend analysis of the precipitation, PET, and runoff series during the past 52 years. The results (Table 2) show that precipitation and PET series have no significant increasing or decreasing trend. While, the runoff series exhibited a significantly decreasing trend (with a positive significance of 0.99) at a rate of 6.3mm every 10 years during the entire study period.

Based on the results of trend analysis, the Pettitt test was selected to identify the change-point for the runoff series. The results (Fig. 5a) show that the first change-point of this series was observed in 1979 (P = 0.99). In addition, the precipitation and runoff double accumulative curve method (DCC) was used to assist in identifying the change-point for the runoff series. The results (Fig. 5b) also show that the gradient of the runoff accumulation curve was significantly different from that of the precipitation accumulation curve after 1979.

After finding the change-point, the social and economic data (Fig. 6) collected from Chifeng city located in the Laohahe basin were analyzed. It was observed that: (1) beginning from 1979, the food production (Fig. 6a) in the city increased rapidly. Similarly, the animal husbandry industry (Fig. 6b) continued to stabilize at a high level after 1979 and experienced rapid growth in the 21st century. These phenomena are closely related to the Chinese land reform conducted in 1978. However, the rapid development of agriculture consumes a large amount of water resources, which are required for irrigation, drinking water for livestock, and other applications. (2) Before the 21st century, the population of Chifeng city (Fig. 6c) was

rapidly growing. In the 21st century, the population growth has slowed down, but remained at a high level, leading to a sustained increase in the demand for domestic water. (3) The GDP of Chifeng city (Fig. 6d) experienced rapid growth after the national economic opening policy was implemented in 1979 (In 2015, the GDP was more than 200 times greater than that of 1979). The secondary and tertiary industries that supported the rapid growth of GDP also caused a massive consumption of water resources.

In addition, the construction and operation of large reservoirs in the Laohahe basin also produced a significant effect on the natural runoff series. Before the 21st century, the Laohahe basin was mainly regulated by two large reservoirs, namely the Erdaohezi (storage capacity: 0.98×10^8 m^3) and Dahushi (storage capacity: 1.2×10^8 m^3), and the total regulated storage capacity of both reservoirs reached 2.0×10^8 m^3. In 2009, when the Sanzuodian reservoir (with a storage capacity of 3.05×10^8 m^3) was built and operated, the reservoir regulation capacity of the Laohahe basin exceeded 5×10^8 m^3. As a result, the large-scale reservoir regulation caused a sharp reduction in the surface water resources. Besides, the land use and cover changed obviously in the study area after 1979. Cropland and built-up land increased substantially while the areas of water body and grassland decrease persistently. Forest land and unused land changed in fluctuation with a decrease on the whole (Yong et al., 2013).

Through analyzing these phenomena, it revealed that the natural hydrological processes of the basin were affected not only by climate change, but also by various human activities after the change-point in 1979 (especially the runoff series, which exhibited a rapidly decreasing trend with a large descending rate).

3.2. Hydrological drought analysis based on traditional assessment methods

In this section, the TLM (Fig. 7a) and SRI (Fig. 7b) methods were used to analyze the hydrological drought occurred in the Laohahe basin during the past 52 years (1964–2015) in a changing environment. Using the former method, a fixed threshold value was calculated for the entire period (1964–2015) and applied to the entire time series. Likewise, 3-month SRI values

(SRI-3) were calculated based on the entire period (1964–2015) using a three-parameter GEV distribution function. These two methods are different from the improved methods described in section 3.2.

The results (Table 3) show that hydrological drought events frequently occurred in the 1980s (1980–1989), 2000s (2000–2009), and 2010s (2010–2015), while in other decades, their frequency was much lower. When TLM was used for drought evolution, 60%, 81%, and 99% of droughts were identified in the 1980s, 2000s, and 2010s, respectively. Similarly, 45%, 58%, and 100% of droughts were detected in the 1980s, 2000s, and 2010s, respectively, using the SRI method.

However, in terms of the drought characteristics (e.g. the number and duration of droughts), the results obtained by the two methods were quite different. Using the TLM method, 9, 12, and 12 drought events were identified in the 1960s, 1970s, and 1990s, while only 2, 1, and 2 drought events were identified in these periods by the SRI method, respectively. Similarly, using the TLM method, the drought durations determined for these three decades were 18 months, 32 months, and 24 months, whereas the drought durations obtained by the SRI method were equal to 2 months, 1 month, and 8 months, respectively. In addition, the deficit volume of the dry decade (e.g., the 1980s, 2000s) was 4 to 9 times larger than that of the humid decade when the TLM method was utilized, while the drought severity showed that the extent of expansion was significantly greater when the SRI method was used (for example, the drought severity in the 1980s was 150 times higher than that in the 1970s).

Then, 3-month standardized precipitation index (SPI-3) values were calculated from the precipitation series (1964–2015) for meteorological drought (Fig. 7c). The meteorological drought process driven by precipitation did not exhibit an obvious inter-annual change in contrast to the runoff-driven hydrological drought process. By comparing the results of the three methods, it can be concluded that the irregularity of hydrological drought is beyond the range of natural drought evolution (since the 21st century, the proportion of drought event was over 80% and even reached 100% in the 2010s). Besides, large differences in the drought

characteristics were obtained by various methods, indicating that the traditional drought assessment methods might produce deviations during the drought identification of basins in a changing environment, especially for the droughts disturbed by intense human activities. Therefore, drought assessment methods must be optimized to distinguish the impacts of climate change and human activities on hydrological drought both accurately and quantitatively.

3.3. Quantifying the impacts of climate change and human activities on hydrological drought

By combining the results of runoff variation analysis and change-point identification performed in section 3.1, the time series of the study period was divided into two parts: the baseline period ("undisturbed") from 1964 to 1979 and the change period ("disturbed") from 1980 to 2015. According to this division, the hydrometeorological forcing data of the baseline period were used to calibrate the VIC model (Fig. 8a), in which 1964 was the warm-up period, 1965–1974 was the calibration period, and the remaining 1975–1979 was the validation period. The values of NSE, BIAS, and CC were 0.83, 5.1%, and 0.92 for the calibration period and 0.73, 2.5%, and 0.86 for the validation period, respectively, which showed that the VIC model could accurately simulate the natural runoff series. After that, the runoff series during the change period were simulated using the calibrated VIC model and meteorological forcing data (Fig. 8b). The difference between the observed and simulated runoff series is mainly a reflection of the impact of human activities, including some minor simulation errors.

Subsequently, we used the two improved methods, namely, TLM_v and SRI_t method to analysis and quantify the impacts of climate change and human activities to hydrological drought. Firstly, we compared the drought characteristics identified from simulated runoff (affected by only climate change) during the "baseline period" (1964–1979) with that during the "change period" (1980–2015) in the Table 4 to analysis the effect of climate change to

hydrological drought using the above two methods. Results show that, when using the TLM_v method, the duration of drought was increased by 1.1–1.6 times, and the deficit volume was increased by 1.8–2 times. Similarly, when using the SRI_t method, the duration of drought was increased by 1.2–1.3 times, and the drought severity was increased by 1.6–2.2 times. It indicated that climate change aggravated hydrological drought slightly during the change period. Then, drought assessment of the observed and simulated runoff series during the change period was carried out through the two improved methods to analysis the effect of human activities to hydrological drought. Using the former method (Table 4, Fig. 9a and Fig. 9b), the number of droughts identified during simulated series (affected by only climate change) was very close to that of the observed ones (affected by both climate change and human activities); however, when human activities were considered, the duration of drought was increased by 3–9 times, and the deficit volume was increased by 4–11 times. Similar results were obtained using the SRI_t method (Table 4, Fig. 10a and Fig. 10b); in this case, the duration of drought increased by 4–12 times and drought severity increased by 8–15 times. Hence, the drought affected by human activities is more serious than natural drought (affected only by climate change).

Fig. 9c and Fig. 10c show the differences between the observed and natural droughts (distinguished from the simulated series), which indicate the impact of the net human activities on the drought; here, the positive value means aggravating drought and the negative value means relieving drought. The contribution of climate change calculated by the TLM_v method accounts only for 20.6–41.2%, while the impact of human activities accounts for 58.8–79.4%. Similarly, the values computed using the SRI_t method are equal to 15.3–45.3% for the climate change and 54.7–84.7% for the human activities.

The results obtained by the two methods indicate that both climate change and human activities aggravated hydrological drought and human activities is the dominant factor

affecting hydrological drought. Moreover, by comparing the results of different decades, it was found that the influence of human activities represents a growing trend (Fig. 11). Precipitation and evaporation are normally recognized as the most crucial climate factors to control runoff, and further affect hydrological drought. In the Laohahe basin, the decreasing trend of evaporation (represented by PET) is smaller than that of precipitation and the difference between these two factors will lead to runoff reduction and further cause more droughts. In addition to the climate change, human activities such as land use/cover changes and reservoir construction will also affect hydrological drought. The area of cropland of the Laohahe basin was 6852 km^2 before the 1980s, and with the continuous increase in land reclamation it reached 7370 km^2 in the 2000s, accounting for about 40% of the total basin area. The areal coverage of grassland dropped from 5882 km^2 in 1980s to 4629 km^2 in the 2000s (Yong et al., 2013). The substantial increase of water-consuming cropland and continuous decrease of grassland contributed serious loss of surface water and hydrological drought. Additionally, reservoir construction with a total storage capacity exceeding 5×10^8 m^3 disrupted the natural hydrological cycle and provided more water supplies for irrigation and domestic water usage, consequently further led to the occurrence of severe hydrological drought events.

3.4. Discussion on the uncertainty of hydrologic simulation

The entire hydrological drought separation framework is based on the hydrological model simulation; hence, the accurate simulation of the hydrological characteristic process line directly affects the results of the hydrological drought assessment. In this study, biases (errors not more than 5.1%, equivalent to approximately 0.14mm/month in runoff) of the VIC model during the baseline period is mainly caused by overestimating or underestimating the runoff peak, while the drought events mostly occur in the dry season (the low-runoff period). The systematic bias caused by the flood peak period does not affect the drought assessment results in any significant way as long as the low-runoff process can be accurately simulated. More directly, we compared the differences in drought characteristics between observations and hydrological model simulations during the baseline period to analyze the propagated bias in

droughts. Results show that (Table 4), when using TLM_v method, the difference of the drought duration is an average of 0.1 months, and the difference of deficit (drought severity) is an average of 0.2mm per drought. Likely, when using SRI_t method, the difference is 0.3months, and 0.3 per drought, respectively. These magnitudes in general are rather small compared with that of human-induced droughts during the change period, where the difference of drought duration and deficit volume (drought severity) are 6.8 months and 8mm per drought using the TLM_v method, and 9.9 months and 21.8 per drought using SRI_t method. In other words, minor errors derived from model simulations though exist; they will not influence the dominant contribution of human activities substantially. In future studies, we can compare the simulation results of multiple hydrological models and use optimization method to reduce uncertainties, including model uncertainty (arising from lumped and simplified representation of hydrological processes in hydrologic models) and parametric uncertainty (reflecting the inability to specify exact values of model parameters due to finite length and uncertainties in the calibration data) (Renard et al., 2010; Jiang et al., 2018a).

4. Conclusion

Hydrological drought is greatly influenced by climate change and human activities in a changing environment. In this paper, we established a separation framework including the TLM_v and SRI_t method to quantify the impacts of climate change and human activities on hydrological drought. The results of the case study conducted for the semiarid Laohahe basin of North China are as follows:

(1) The traditional drought assessment methods were used to identify hydrological drought of the Laohahe basin between 1964 and 2015. The obtained results showed that the hydrological drought in the basin exhibited an apparent irregularity and was beyond the range of the natural drought evolution. Because of the significant impacts of human activities on the hydrological process, the traditional hydrological drought assessment methods are no longer applicable to some basin in a changing environment.

(2) Through the MK test, the precipitation and PET series exhibits no apparent downward

trend, while the runoff series demonstrates a rapidly decreasing trend. The first change-point for the Laohahe basin determined by the Pettitt test is dated 1979. The analysis of multiple economic indicators of Chifeng city located in the Laohahe basin, land use changes, and reservoir construction reveal that various forms of human activities have had a significant impact on the hydrological process since 1979, which also confirmed the results of the change-point test.

(3) The hydrological drought during the change period (1980-2015) in the Laohahe basin was evaluated using the proposed separation framework. The results show that when human activities are considered, the duration of the drought is increased by 3–9 times using the TLM_v method and by 4–12 times using the SRI_t method respectively. The increases in the deficit volume amount to 4–11 times using TLM_v method, and the drought severity expands by 8–15 times through the SRI_t method, indicating that the degree of drought severity resulting from human activities is greater than that corresponding to natural drought.

(4) The impacts of climate change and human activities on hydrological drought were quantified. The results obtained by the TLM_v method show that climate change accounted for 20.6–41.2% of the total impact, and human activities accounted for 58.8–79.4%. For comparison, the results obtained by the SRI_t method demonstrate that climate change accounted for 15.3–45.3% of the total impact, and human activities accounted for 54.7–84.7%. The results from the two methods indicate that both climate change and human activities aggravated hydrological drought and human activities are the dominant factor affecting hydrological drought with an upward trend.

Acknowledgement

The current study was jointly supported by the National Key Research and Development Program approved by Ministry of Science and Technology, China (2016YFA0601504); the Program of Introducing Talents of Discipline to Universities by the Ministry of Education and the State Administration of Foreign Experts Affairs, China (B08048); the National Natural Science Foundation of China (41501017, 51779070), the Natural Science Foundation of

Jiangsu Province (BK20150815), the Fundamental Research Funds for the Central Universities (2019B10414), and the Research Council of Norway (FRINATEK Project 274310).

References

Allen RG, Pereira LS, Raes D, Smith M. (1998). Crop Evapotranspiration: Guidelines for Computing Crop Water Requirements. *United Nations Food and Agriculture Organization, Irrigation and Drainage Paper*, 56.

Bazrafshan, J., & Hejabi, S. (2018). A Non-Stationary Reconnaissance Drought Index (NRDI) for Drought Monitoring in a Changing Climate. *Water Resources Management*, 32, 2611–2624.

Dai, A. G. (2011). Drought under global warming: a review. *Wiley Interdisciplinary Reviews: Climate Change*, 2(1), 45–65.

Dai, A. G. (2013). Increasing drought under global warming in observations and models. *Nature Climate Change*, 3(1), 52–58.

Firoz, A. B. M., Nauditt, A., Fink, M., & Ribbe, L. (2018). Quantifying human impacts on hydrological drought using a combined modelling approach in a tropical river basin in central Vietnam. *Hydrology and Earth System Sciences*, 22, 547–565.

Haro-Monteagudo, D., Daccache, A., & Knox, J. (2018). Exploring the utility of drought indicators to assess climate risks to agricultural productivity in a humid climate. *Hydrology Research*, 49 (2), 539-551.

Han, S. J., Tang, Q. H., Xu, D., & Wang, S. L. (2014). Irrigation-induced changes in potential evaporation: moreattention is needed. *Hydrological Processes*, 28, 2717–2720.

Heim, R. R. (2002). A review of twentieth-century drought indices used in the United States. *Bulletin of the American Meteorological Society*, 83(8), 1149–1165.

He, X., Wada, Y., Wanders, N., & Sheffield, J. (2017). Human water management intensifies hydrological drought in California. *Geophysical Research Letter*, 44, 1777–1785.

Jiang, S. H., Ren, L. L., Yong, B., Singh, V. P., Yang, X. L., & Yuan, F. (2011). Quantifying the effects of climate variability and human activities on runoff from the Laohahe basin in

northern China using three different methods. *Hydrological Processes*, 25, 2492–2505.

Jiang, S. H., Ren, L. L., Yong, B., Fu, C. B., & Yang, X. L. (2012a). Analyzing the effects of climate variability and human activities on runoff from the Laohahe basin in northern China. *Hydrology Research*, 43(1-2), 3-13.

Jiang S. H., Ren, L. L., Hong, Y., Yong, B., Yang, X. L., Yuan, F., & Ma, M. W. (2012b). Comprehensive Evaluation of Multi-satellite Precipitation Products with a Dense Rain Gauge Network and Optimally Merging their Simulated Hydrological Flows using the Bayesian Model Averaging Method. *Journal of Hydrology*, 452-453, 213-225.

Jiang, S. H., Ren, L. L., Xu, C.-Y., Liu, S. Y., Yuan, F., & Yang, X. L. (2018a). Quantifying multi-source uncertainties in multi-model predictions using the Bayesian model averaging scheme. *Hydrology Research*, 49(3), 954-970.

Jiang S. H., Ren, L. L., Xu, C.-Y., Yong, B., Yuan, F., Liu, Y., Yang, X. L., & Zeng, X. M. (2018b). Statistical and Hydrological Evaluation of the Latest Integrated Multi-satellitE Retrievals for GPM (IMERG) over a Midlatitude Humid Basin in South China. *Atmospheric Research*, 214, 418-429.

Kendall, M. G. (1975). Rank correlation methods. Charles Griffin, London.

Kiely, G., Albertson, J. D., & Parlange, M. B. (1998). Recent trends in diurnal variation of precipitation at Valentia on the west coast of Ireland. *Journal of Hydrology*, 207, 270–279.

Li, Y., Chen, C., & Sun, C. (2017). Drought severity and change in Xinjiang, China, over 1961–2013. *Hydrology Research*, 48, 1343-1362.

Liang, X., Guo, J., & Leung, L. R. (2004). Assessment of the effects of spatial resolutions on daily water flux simulation. *Journal of Hydrology*, 298, 287–310.

Liang, X., Lettenmaier, D. P., Wood, E. F., & Burges, S. J. (1994). A simple hydrologically based model of land surface water and energy fluxes for GSMs. *Journal of Geophysical Research: Atmospheres*, 99(D7), 14415–14428.

Lin, Q. X., Wu, Z. Y., Singh, V. P., Sadeghi, S. H. R., He, H., & Lu, G. H. (2017). Correlation between hydrological drought, climatic factors, reservoir operation, and vegetation cover in the Xijiang Basin, South China. *Journal of Hydrology*, 549, 512-524.

Liu, X. F., Ren, L. L., Yuan, F., Singh, V. P., Fang, X. Q., Yu, Z. B., & Zhang, W. (2009). Quantifying the effect of land use and land cover changes on green water and blue water in northern part of china. *Hydrology and Earth System Sciences*,13, 735-747.

Liu, Y., Ren, L. L., Zhu, Y., Yang, X. L., Yuan, F., Jiang, S. H., & Ma, M. W. (2016). Evolution of Hydrological Drought in Human Disturbed Areas: A Case Study in the Laohahe Catchment, Northern China. *Advances in Meteorology*, 2016, 1-12.

Ma, M. W., Ren, L. L., Yuan, F., Jiang, S. H., Liu, Y., Kong, H., & Gong, L. Y. (2014). A new standardized Palmer drought index for hydro-meteorological use. *Hydrological Processes*, 28, 5645–5661.

Mann, H. B. (1945). Nonparametric tests against trend. *Econometrica: Journal of the Econometric Society*, 13, 245–259.

Mishra, A. K., & Singh, V. P. (2010). A review of drought concepts. *Journal of Hydrology*, 391, 202-216.

Nalbantis, I., & Tsakiris, G. (2009). Assessment of hydrological drought revisited. *Water Resources Management*, 23, 881–897.

Pettitt, A. N. (1979). A non-parametric approach to the change-point problem. *Journal of the Royal Statistical Society. Series C (Applied Statistics)*, 28(2), 126-135.

Razmkhah, H. (2017). Comparing Threshold Level Methods in Development of Stream Flow Drought Severity-Duration-Frequency Curves. *Water Resources Management*, 31, 4045-4061.

Ren, L. L., Wang, M. R., Li, C. H., & Zhang, W. (2002). Impacts of human activity on river runoff in the northern area of China. *Journal of Hydrology*, 261, 204–217.

Ren, L. L., Shen, H. R., Yuan, F., Zhao, C. X., Yang, X. L., & Zheng, P. L. (2016). Hydrological drought characteristics in the Weihe catchment in a changing environment. *Advances in Water Science*, 27(4), 492–500. (in Chinese)

Renard, B., Kavetski, D., Kuczera, G., Thyer, M., & Franks, S. W. (2010). Understanding predictive uncertainty in hydrologic modeling: the challenge of identifying input and structural errors. *Water Resources Research*, 46(5), 1187-1191.

Rivera, J. A., Araneo, D. C., Penalba, O. C., & Villalba, R. (2018). Regional aspects of streamflow droughts in the Andean rivers of Patagonia, Argentina. Links with large-scale climatic oscillations. *Hydrology Research*, 49 (1), 134-149.

Safavi, H. R., Raghibi, V., Mazdiyasni, O., & Mortazavi-Naeini, M. (2018). A new hybrid drought-monitoring framework based on nonparametric standardized indicators. *Hydrology Research*, 49 (1), 222-236.

Sarailidis, G., Vasiliades, L., Loukas, A. (2018). Analysis of streamflow droughts using fixed and variable thresholds. *Hydrological Processes*, 2018, 1–18.

Sheffield, J., Wood, E. F., & Roderick, M. L. (2012). Little change in global drought over the past 60 years. *Nature*, 491(7424), 435–438.

Shukla, S., & Wood, A. W. (2008). Use of a standardized runoff index for characterizing hydrologic drought. *Geophysical Research Letter*, 35(2), 226–236.

Tijdeman, E., Hannaford, J., & Stahl, K. (2018). Human influences on streamflow drought characteristics in England and Wales. *Hydrology and Earth System Sciences*, 22, 1051–1064.

Trenberth, K. E., Dai, A. G., Schrier, G., Jones, P. D., Barichivich, J., Briffa, K. R., & Sheffield, J. (2014). Global warming and changes in drought. *Nature Climate Change*, 4, 17–22.

Van Loon, A. F., & Van Lanen, H. A. J. (2013). Making the distinction between water scarcity and drought using an observation-modeling framework. *Water Resources Research*, 49, 1483–1502.

Van Loon, A. F. (2015). Hydrological drought explained. *WIREs Water*, 2, 359–392.

Van Loon, A. F., Gleeson, T., Clark, J., Van Dijk, A. I. J. M., Stahl, K., Hannaford, J., Baldassarre, G. D., Teuling, A. J., Tallaksen, L. M., Uijlenhoet, R., Hannah, D. M., Sheffield, J., Svoboda, M, Verbeiren, B., Wagener, T., Rangecroft, S., Wanders, N., & Van Lanen, H. A. J. (2016). Drought in the Anthropocene. *Nature Geoscience*, 9, 89–91.

Vicente-Serrano, S. M., Schrier, G. V., Begueria, S., Azorin-Molina, C., & Lopez-Moreno, J. I. (2015). Contribution of precipitation and reference evapotranspiration to drought indices under different climates. *Journal of Hydrology*, 526, 42–54.

Wan, W., Zhao, J., Li, H. Y., Mishra, A., Ruby Leung, L., Hejazi, M., Wang W., Lu, H., Deng, Z. Q., Demissisie, Y., & Wang, H. (2017). Hydrological drought in the anthropocene: Impacts of local water extraction and reservoir regulation in the U.S. *Journal of Geophysical Research: Atmospheres*, 122, 11313–11328.

Wang, Z. L., Zhong, R. D., Lai, C. G., Zeng, Z. Y., Lian, Y.Q., & Bai, X. Y. (2018). Climate change enhances the severity and variability of drought in the Pearl River Basin in South China in the 21st century. *Agricultural and Forest Meteorology*, 249, 149–162.

Ye, X. C., Li, X. H., Xu, C.-Y., & Zhang, Q. (2016). Similarity, difference and correlation of meteorological and hydrological drought indices in a humid climate region-the Poyang lake catchment in China. *Hydrology Research*, 47(6), 1211-1223.

Yong, B., Ren, L. L., Hong, Y., Gourley, J. J., Chen, X., Dong, J.W., Wang, W. G., Shen, Y., & Hardy, J. (2013). Spatial–Temporal Changes of Water Resources in a Typical Semiarid Basin of North China over the Past 50 Years and Assessment of Possible Natural and Socioeconomic Causes. *Journal of Hydrometeorology*, 14, 1009–1034.

Yu, M. X., Li, Q. F., Hayes, M. J., Svoboda, M. D., & Heim, R. R. (2014). Are droughts becoming more frequent or severe in China based on the Standardized Precipitation Evapotranspiration Index: 1951–2010? *International Journal of Climatology*, 34, 545–558.

Zhang, D., Zhang, Q., Qiu, J. M., Bai, P., Liang, K., & Li, X. H. (2018). Intensification of hydrological drought due to human activity in the middle reaches of the Yangtze River, China. *Science of the Total Environment*, 637-638, 1432–1442.

Zhu, Y., Wang, W., Singh, V. P., & Liu, Y. (2016). Combined use of meteorological drought indices at multi-time scales for improving hydrological drought detection. *Science of the Total Environment*, 571, 1058–1068.

Zhu, B. W., Xie, X. H., & Zhang, K. (2018). Water storage and vegetation changes in response to the 2009/10 drought over North China. *Hydrology Research*, 49 (5), 1618-1635.

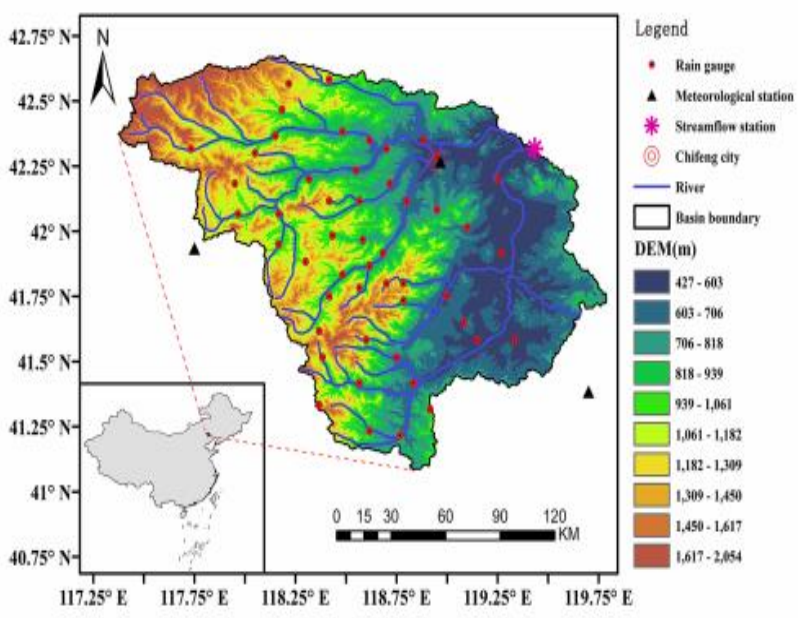

Fig. 1. Location of the study area and distributions of the rain gauges, meteorological stations, and Xinlongpo hydrologic station.

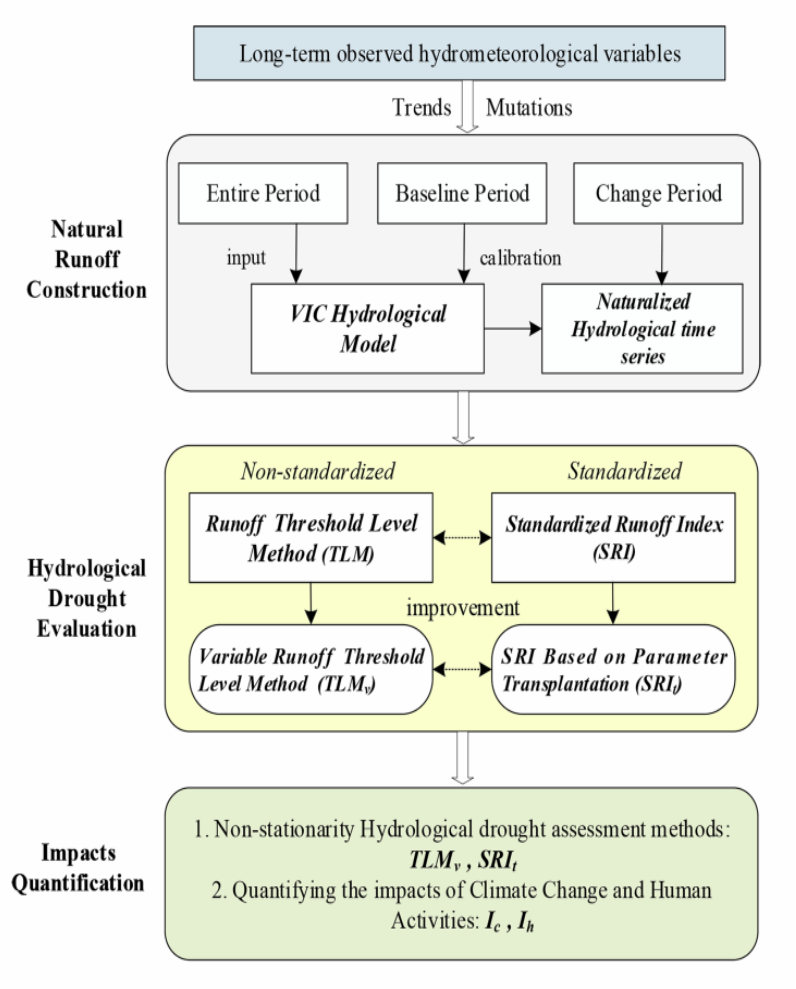

Fig. 2. Hydrological drought evaluation framework.

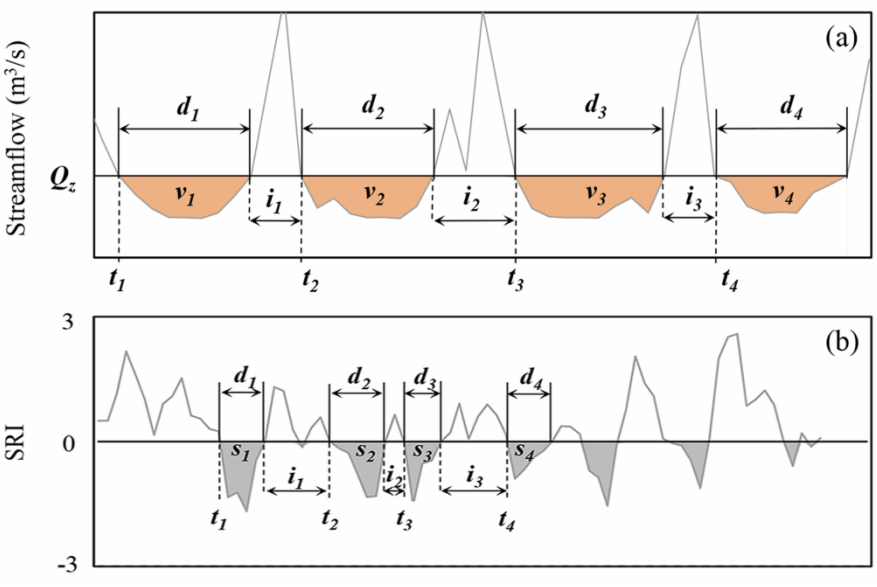

Fig. 3. Illustrations of (a) the TLM method (time of occurrence, t_k, duration, d_k, deficit volume, v_k, drought interval, i_k, and the threshold level, Q_z) and (b) the SRI method (time of occurrence, t_k, duration, d_k, drought severity, s_k, drought interval, i_k).

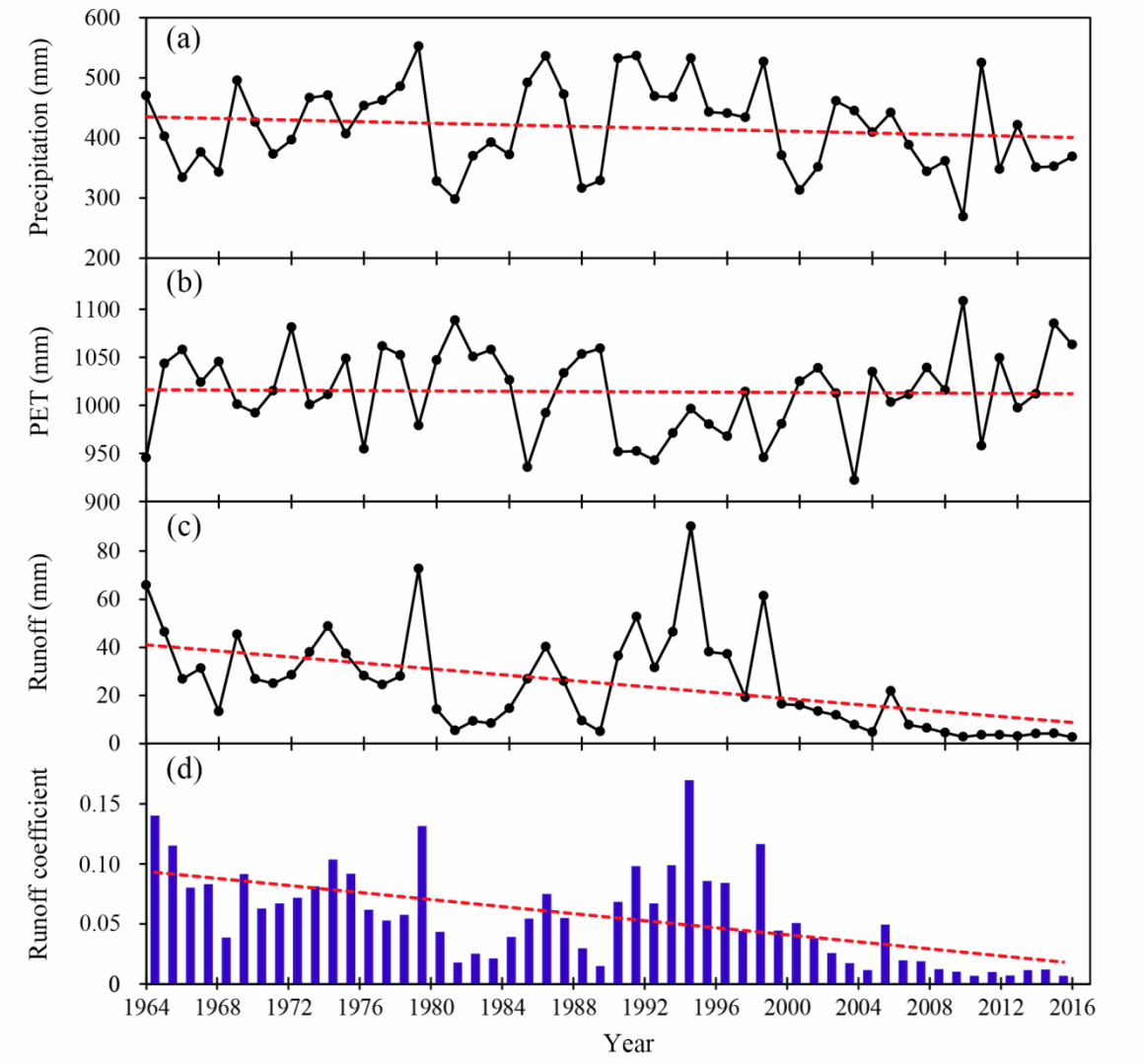

Fig. 4. Variations of the (a) annual precipitation, (b) PET, (c) runoff, and (d) runoff coefficient observed for the Laohahe catchment since 1964. The red dashed lines denote the corresponding linear trends.

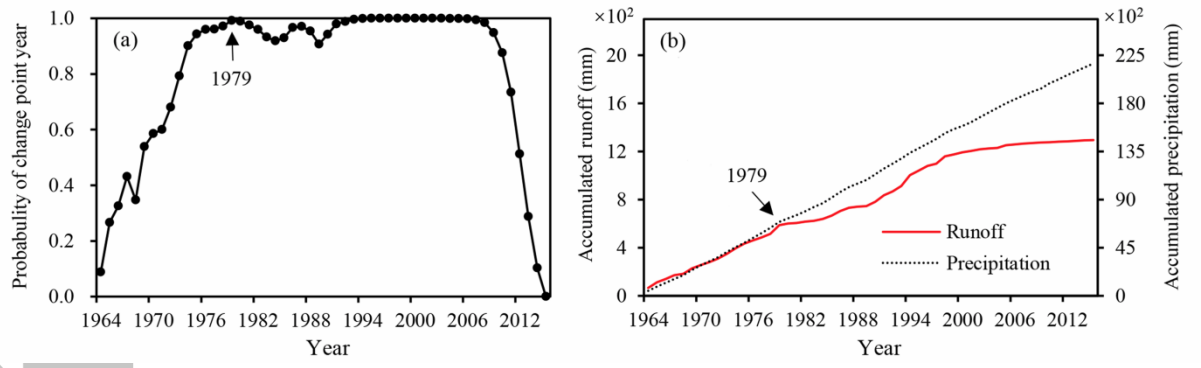

Fig. 5. (a) Probability of a change-point year and (b) double cumulative curves of the annual precipitation and runoff.

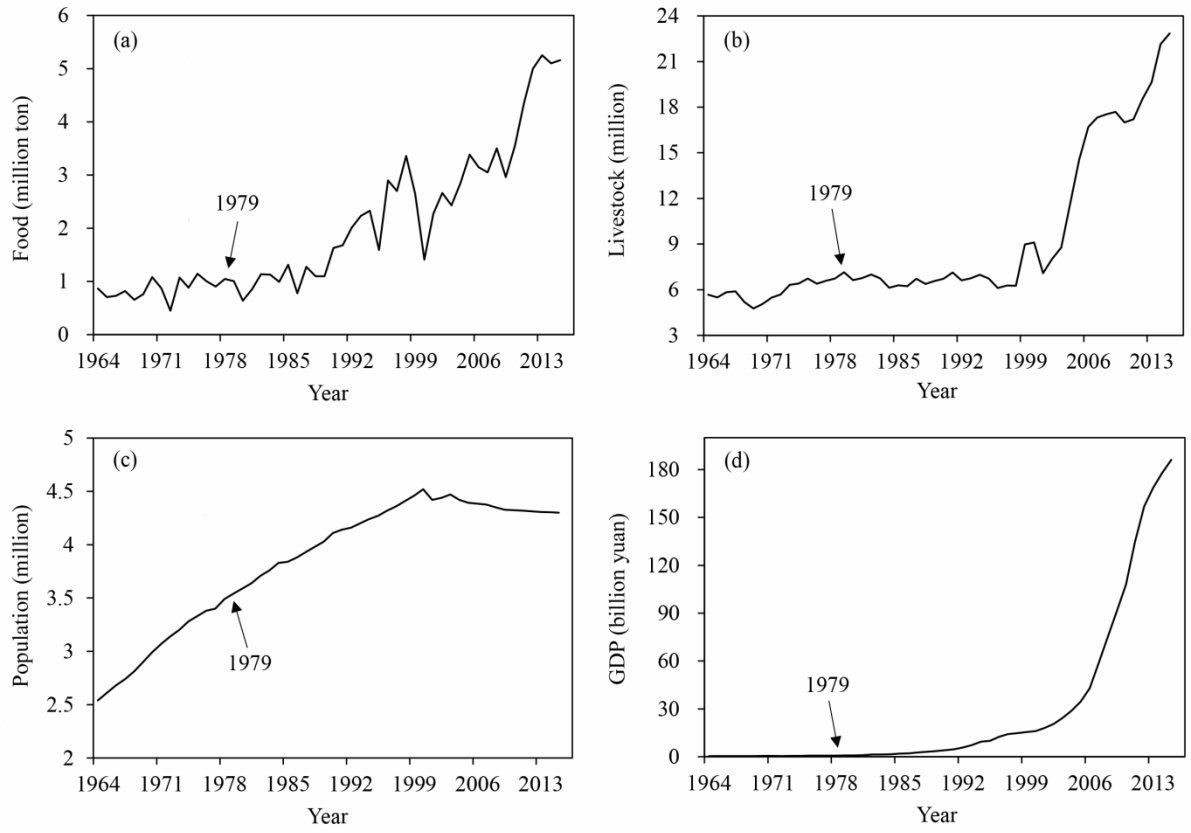

Fig. 6. Changes in the quantities of (a) food, (b) livestock, (c) population, and (d) GDP for Chifeng city in 1964–2015.

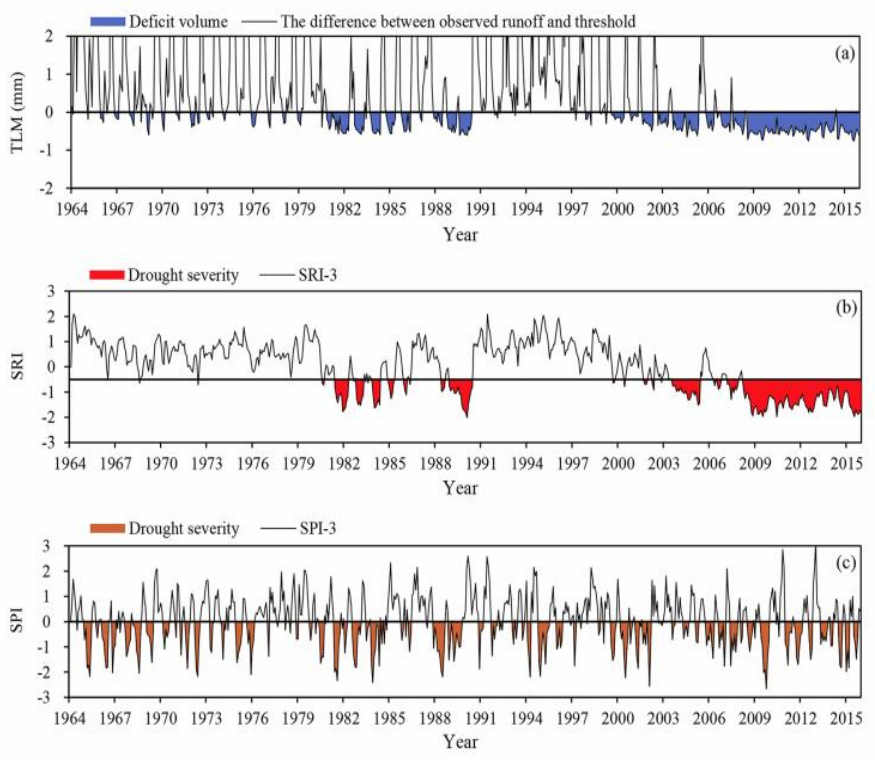

Fig. 7. Temporal evolutions of the (a) hydrological drought identified using the TLM method (derived from the runoff series), (b) hydrological drought identified using the SRI method (derived from the runoff series), and (c) meteorological drought identified using the SPI method (derived from the precipitation series).

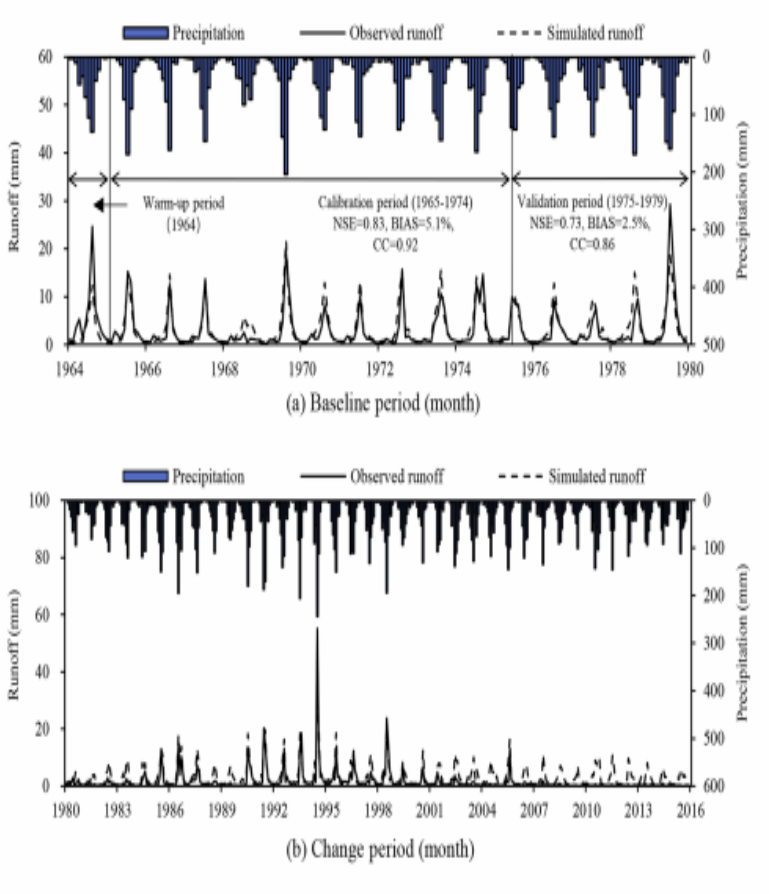

Fig. 8. VIC simulated monthly runoff at the Xinlongpo hydrologic station for the (a) baseline period of 1964–1979 and (b) change period of 1980–2015.

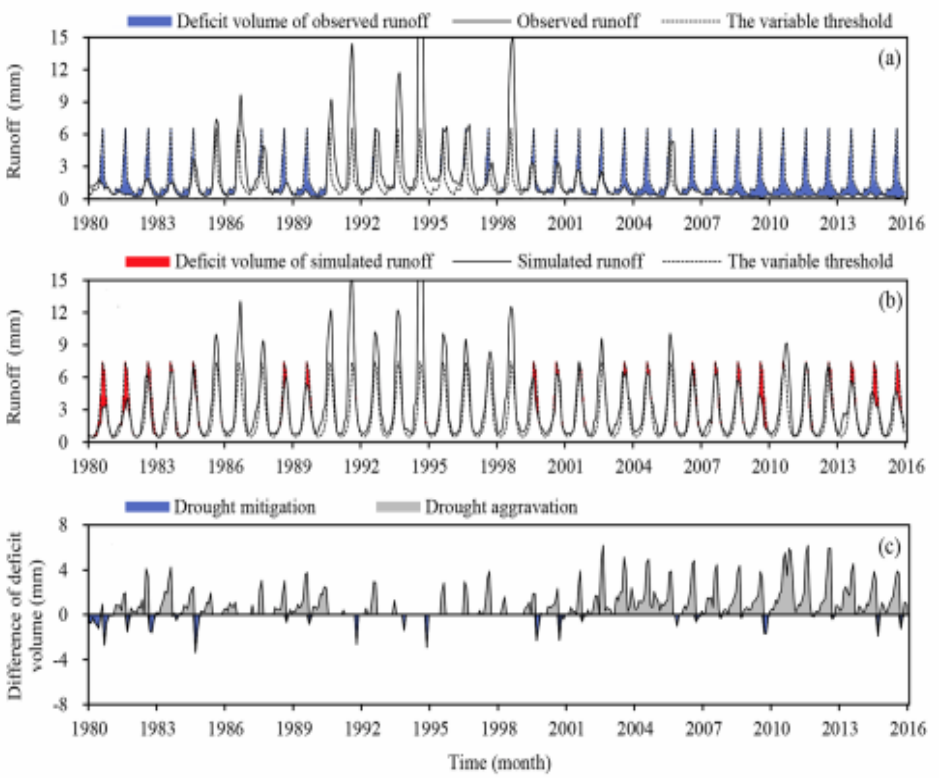

Fig. 9. Hydrological droughts identified with the TLM_v method during 1980–2015 from the (a) observed and (b) simulated runoff series. (c) Difference of deficit volume between the observed and simulated runoff series representing the net effect of human activities on hydrological drought.

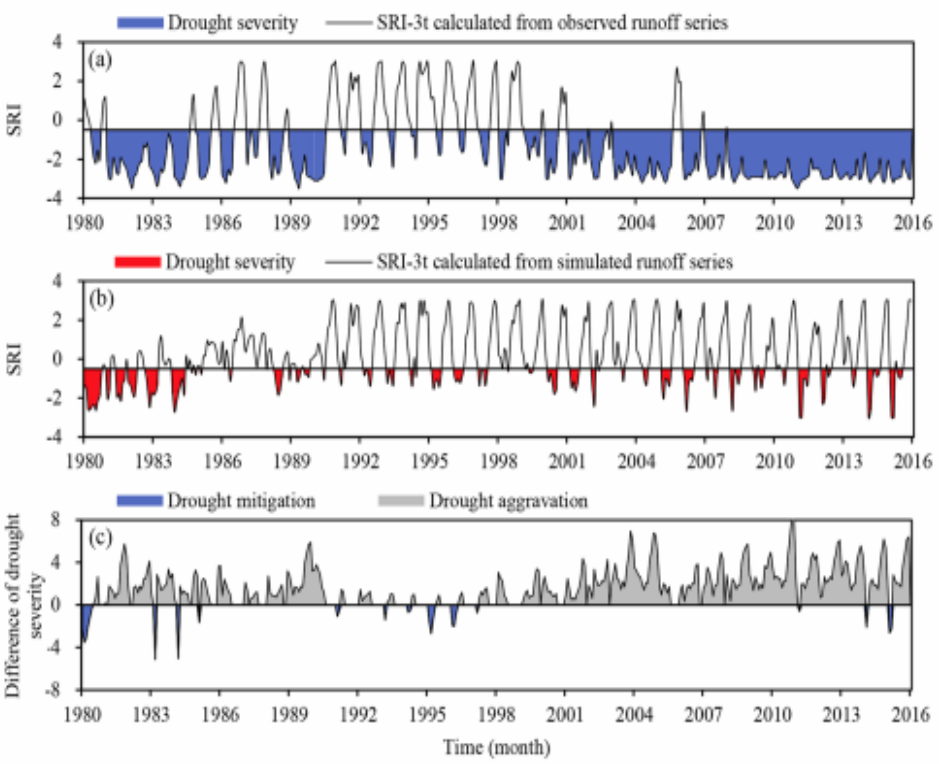

Fig. 10. Hydrological droughts identified with the SRI_t method during 1980–2015 from the (a) observed and (b) simulated runoff series. (c) Difference of drought severity between the observed and simulated runoff series representing the net effect of human activities on hydrological drought.

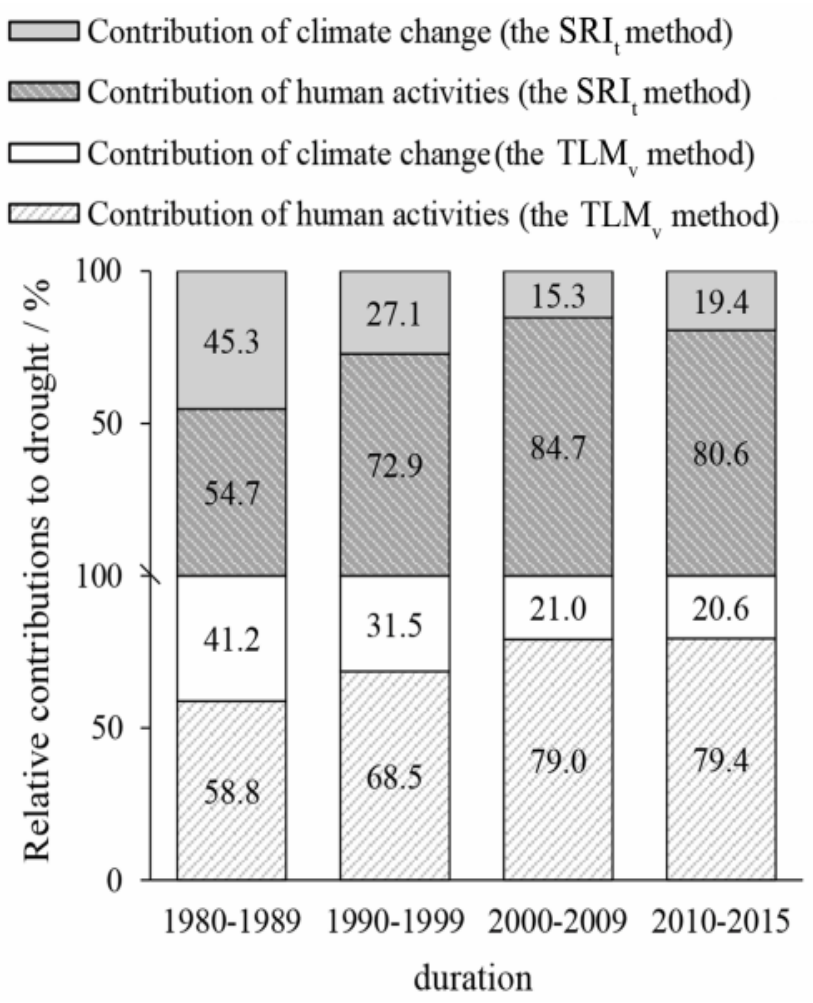

Fig. 11. Relative contributions of climate change and human activities to hydrological drought calculated by two different methods.

Table 1

Seven parameters commonly calibrated in the VIC-3L model, their physical meanings, and default values.

Parameter	Physical meaning	Unit	Numeric range	Default parameter value
B	Infiltration curve parameter	N/A	0–0.4	0.01
d_2	Thickness of the middle soil moisture layer	m	0–2	1.35
D_s	Fraction of D_{smax} where the non-linear baseflow begins	Fraction	0–1	0.004
D_{smax}	Maximum velocity of the baseflow	mm/day	0–30	6
W_s	Fraction of the maximum soil moisture where non-linear baseflow occurs	Fraction	0–1	0.98
d_1	Thickness of the top thin soil moisture layer	m	0.05–0.1	0.05
d_3	Thickness of the lower soil moisture layer	m	0–2	2

Table 2

Trend and change-point analysis of the annual precipitation, PET, and runoff.

Factor	Mean value (mm/a)	Trend rate (mm/10a)	MK trend test		Pettitt change-point analysis
			Z	Positive significance	
Precipitation	417.9	–6.7	–1.27	—	—
PET	1014.1	–0.8	–0.13	—	—
Runoff	24.9	–6.3	–4.80	0.99	1979

Table 3

Hydrological drought characteristics identified from observed runoff using TLM and SRI method, and meteorological drought characteristics identified from observed precipitation using SPI method during 1964-2015.

Period	Number of droughts			Duration (months)			Deficit（mm）/ Drought severity		
	TLM	SRI	SPI	TLM	SRI	SPI	TLM	SRI	SPI
1964–1969	9	2	8	18	2	26	3.7	0.2	18.5
1970–1979	12	1	15	32	1	26	7.1	0.2	16.6
1980–1989	13	12	18	72	54	43	28.1	33.0	31.5
1990–1999	12	2	15	24	8	24	4.6	5.5	16.7
2000–2009	10	10	21	97	70	45	33.8	39.8	26.1
2010–2015	2	1	11	71	72	27	35.2	64.3	16.4

TLM, the runoff threshold level method; SRI, the standardized runoff index method; SPI, the standardized precipitation index method.

Table 4

Drought characteristics identified from observed and simulated runoff using TLM_v and SRI_t method during 1964-2015.

Period	Method	Series	Number of droughts	Duration (month)		Deficit volume(mm)/ drought severity	
				Mean	Max	Mean	Max
Baseline period (1964-1979)	TLM_v	Observed	14	3.0	6	1.9	5.6
		Simulated	17	2.9	7	1.7	6.2
	SRI_t	Observed	14	3.2	8	2.4	5.2
		Simulated	20	2.9	6	2.1	6.9
Change period (1980-2015)	TLM_v	Observed	29	9.9	94	11.2	131.8
		Simulated	34	3.1	11	3.2	12.5
	SRI_t	Observed	24	13.3	96	25.2	225.7
		Simulated	47	3.4	8	3.4	15.0

TLM_v, the variable runoff threshold level method; SRI_t, the Standard Runoff Index based on parameter transplantation.